Decay of a nonlinear impurity in a structured continuum from a nonlinear Fano-Anderson model

Stefano Longhi

Dipartimento di Fisica e Istituto di Fotonica e Nanotecnologie del CNR, Politecnico di Milano,
Piazza Leonardo da Vinci 32, I-20133 Milan, Italy
(Received 4 January 2007; revised manuscript received 22 March 2007; published 18 May 2007)

The decay dynamics of a nonlinear impurity mode embedded in a linear structured continuum is theoretically investigated in the framework of a nonlinear Fano-Anderson model. A gradient flow dynamics for the survival probability is derived in the Van Hove ($\lambda^2 t$) limit by a multiple-scale asymptotic analysis, and the role of nonlinearity on the decay law is discussed. In particular, it is shown that the existence of bound states embedded in the continuum acts as transient trapping states which slow down the decay. The dynamical behavior predicted in the $\lambda^2 t$ limit is studied in detail for a simple tight-binding one-dimensional lattice model, which may describe electron or photon transport in condensed matter or photonic systems. Numerical simulations of the underlying equations confirm, in particular, the trapping effect in the decay process due to bound states embedded in the continuum.

PACS number(s): 73.20.Hb, 03.65.Ge, 73.23.−b, 05.60.Gg

I. INTRODUCTION

The description of the decay dynamics of unstable quantum states is a subject of considerable and continuous relevance in different areas of physics.[1–3] It is well known that an exponential decay law is the universal hallmark of unstable systems according to the Fermi golden rule, whose quantum-mechanical derivation is based on the assumption that the temporal evolution of an unstable quantum system is dominated by a pole near the real axis of the complex energy plane (Weisskopf-Wigner or Breit-Wigner approximation; see, for instance, Ref. 4 and references therein). The derivation of an irreversible master equation, characterized by an exponential decay, was rigorously presented in 1950 by Van Hove in an asymptotic analysis based on the so-called $\lambda^2 t$ limit,[2,5,6] which assumes an infinitesimal small coupling λ of the decaying discrete state with the continuum (reservoir) and observes the system on the long time scale $\sim 1/\lambda^2$. However, it is well known that the decay dynamics of an unstable quantum system described by an unitary operator cannot be purely exponential, with deviations from an exponential decay occurring at both short and long times. In particular, at short times, the survival probability $P(t)$ is always parabolic, i.e., $dP/dt \to 0$ as $t \to 0$, a circumstance which can be exploited to slow down the decay process by repetitive measurements (quantum Zeno effect; see, for instance, Refs. 2 and 7 and references therein). Nevertheless, in most common unstable quantum systems encountered in nature, deviations from an exponential decay occur solely at very short or very long times, making it practically impossible their detection; for instance, the Zeno region, i.e., the initial temporal interval where $[dP(t)/dt]/P$ is much smaller than the golden-rule decay rate, may range from $\sim 10^{-17}$ s for spontaneous emission of atoms in vacuum to less than $\sim 10^{-20}$ s for decaying particles (see, for instance, Ref. 4). A way to enhance nonexponential features of the decay dynamics is to "structure" the continuum (reservoir), making the dynamics strongly non-Markovian. Such a possibility has been extensively investigated in recent years especially in the quantum optics context, such as in several studies of spontaneous emission in photonic crystals.[8–10] Typical features of non-Markovian dynamics are nonexponential decay, fractional decay and population trapping, atom-photon bound states, and damped Rabi oscillations. Convincing experimental evidences of these effects in the quantum optics context, however, are still lacking.[11] On the other hand, a typical quantum effect such as the tunnel effect, which is particularly suited to account for the dynamics of unstable systems,[12] can be properly engineered in macroscopic systems in such a way to push the time window of the Zeno region to a measurable level. For such reasons, the first clear experimental observation of nonexponential decay at short times for an unstable system was performed solely one decade ago in an experiment on quantum tunneling of ultracold sodium atoms in an accelerated periodic optical potential,[13] with the Zeno temporal region falling in the microseconds time scale. The observation of Zeno and anti-Zeno effects has been subsequently demonstrated for the same system.[14] Some recent theoretical works have shown that nonexponential decay features and Zeno dynamics also occur for quantum tunneling in other macroscopic or mesoscopic systems, such as Josephson junctions,[15] semiconductor nanostructures,[16] and spin chains,[17] or in photon tunneling in coupled optical waveguides or resonators.[18,19] In many of these systems, nonlinear effects may be non-negligible, and the dynamics should be described by extended Hamiltonian models which properly account for either local or distributed nonlinearity (see, for instance, Refs. 20–31 and references therein). A few relevant examples of nonlinear effects that may accompany tunneling processes are atom-atom interaction in dense matter wave systems,[20–22] polaronic behavior in strongly coupled electron-vibration systems,[23–26] or material nonlinearity in coupled optical waveguides or photonic crystal resonators.[27–31] While the decay dynamics of an unstable state in a linear system, including the validity of the golden rule in the $\lambda^2 t$ limit and the occurrence of nonexponential deviations at short and long times, is to date well understood, the effects of nonlinearity on the decay dynamics have not

received an adequate attention yet. It is the aim of the present work to provide some insights into this subject and to highlight the occurrence of nonexponential features of the decay law which are of purely nonlinear nature. Specifically, we consider the decay dynamics of a *nonlinear discrete state* embedded into a structured linear continuum in the framework of a nonlinear extension of the Fano-Anderson model,[32,33] which may describe electron or photon transport in one-dimensional lattices with a local nonlinear impurity mode.[25,26,29,30,34,35] By means of a multiple-scale asymptotic analysis, a decay law for the survival probability $P(t)$ is derived which provides an extension to the nonlinear case of the $\lambda^2 t$ Van Hove limit.[2,5,6] In the linear regime, the $\lambda^2 t$ limit yields a purely exponential decay (golden rule); the nonlinearity introduces nonexponential features which should be observable whenever the nonlinear-induced shift of the impurity mode resonance spans a spectral region where the reservoir spectral function changes rapidly. A noteworthy case is that of a reservoir spectral function showing pointlike gaps, which induce a slowing down of the decay and a characteristic staircase profile for the survival probability. Such a behavior is closely related to the existence of bound states embedded in the continuum, which are responsible for fractional decay in the linear regime but that are unstable attractors of the dynamics in the nonlinear regime.

The paper is organized as follows. In Sec. II, the nonlinear Fano-Anderson model is presented, and the existence of nonlinear bound states is discussed. In Sec. III, a multiple-scale asymptotic analysis of the underlying equations is used to derive a gradient flow describing the decay dynamics in the $\lambda^2 t$ limit. In particular, it is shown that bound states embedded in the continuum correspond to unstable trapping states which slow down the decay process. In Sec. IV, an example of nonlinear decay dynamics for a tight-binding lattice model with a local impurity is presented, and the main results predicted within the $\lambda^2 t$ asymptotic limit are confirmed by direct numerical simulations of the underlying equations. Finally, in Sec. V, the main conclusions are outlined.

II. NONLINEAR FANO-ANDERSON MODEL

A. Basic model

The starting point of the analysis is provided by an extension of the standard Fano-Anderson model[3,32,33] which describes the interaction of a nonlinear impurity state $|a\rangle$ with a structured linear continuum composed by a set of continuous states $|k\rangle$ with energy $\hbar\omega(k)$. The Hamiltonian of the interacting system can be written as $H = H_0 + \lambda V + H_{NL}$, where

$$H_0 = \hbar\omega_a |a\rangle\langle a| + \int dk\, \hbar\omega(k)|k\rangle\langle k| \qquad (1)$$

is the Hamiltonian of the noninteracting discrete and continuous states in the linear regime (with $\langle a|a\rangle = 1$, $\langle k'|k\rangle = \delta(k'-k)$, and $\langle a|k\rangle = 0$),

$$V = \hbar \int dk[v(k)|a\rangle\langle k| + v^*(k)|k\rangle\langle a|] \qquad (2)$$

describes the interaction of the discrete state $|a\rangle$ with the continuum, λ is a dimensionless parameter that measures the strength of the interaction, and H_{NL} accounts for the nonlinearity localized at the impurity. A typical form of H_{NL} is the following one (see, for instance, Refs. 25 and 35):

$$H_{NL} = -\hbar\gamma f(|c_a|^2)|a\rangle\langle a|, \qquad (3)$$

where $f(|c_a|^2)$ determines the nature of the nonlinearity, γ measures the strength of the nonlinearity, $c_a = \langle a|\psi\rangle$, and $|\psi\rangle$ is the state of the system. In this work, we will assume $f(|c_a|^2) = |c_a|^2$, which corresponds in the condensed-matter context to an underlying harmonic oscillator degree of freedom enslaved to the excitation (electron) at the impurity site,[25] or to a Kerr nonlinearity (e.g., a cubic nonlinear resonator or waveguide) in the optical context.[29,30,36] For the sake of definiteness, in the following we will assume $\gamma > 0$, though a similar analysis could be done for the opposite $\gamma < 0$ case. If we expand the wave function $|\psi\rangle$ of the system as $|\psi\rangle = c_a(t)|a\rangle + \int dk\, c(k,t)|k\rangle$, from the equation $i\hbar\partial_t|\psi\rangle = H|\psi\rangle$, the following coupled-mode equations can be derived for the expansion coefficients $c_a(t)$ and $c(k,t)$:

$$i\dot{c}_a(t) = (\omega_a - \gamma|c_a|^2)c_a + \lambda \int dk\, v(k)c(k,t), \qquad (4)$$

$$i\dot{c}(k,t) = \omega(k)c(k,t) + \lambda v^*(k)c_a(t), \qquad (5)$$

where the dot indicates the derivative with respect to time. Note that, as compared to the standard linear Fano-Anderson model, the localized nonlinearity in the system just introduces a *nonlinear shift* of the resonance frequency ω_a of the impurity state, with the instantaneous nonlinear resonance frequency being $\omega_a^{NL} = \omega_a - \gamma|c_a(t)|^2$. Note that, as in the linear model, from Eqs. (4) and (5), it follows that the norm $\|\psi(t)\|^2$ is conserved, i.e., $\|\psi(t)\|^2 = |c_a(t)|^2 + \int dk|c(k,t)|^2 = 1$. Typically, we assume that the frequency $\omega(k)$ of continuous states spans a finite interval (a band) $\omega_1 < \omega < \omega_2$ for the allowed values of the continuous variable k, and that ω_a^{NL} is fully embedded in the continuum during the dynamics. At initial time $t=0$, we further assume that the system is in state $|a\rangle$, i.e., that $c_a(0) = 1$ and $c(k,0) = 0$. As in the linear Fano-Anderson model, an equivalent formulation of the decay problem can be stated in terms of an integrodifferential equation for $c_a(t)$ solely, which can be derived after an elimination of the continuum degrees of freedom. In fact, substitution of the formal solution $c(k,t)$ obtained from Eq. (5) with the initial condition $c(k,0) = 0$ into Eq. (4) yields the following exact nonlinear Volterra integrodifferential equation for $c_a(t)$:

$$i\dot{c}_a(t) = (\omega_a - \gamma|c_a(t)|^2)c_a(t) - i\int_0^t dt'\,\Phi(t-t')c_a(t'), \quad (6)$$

where

$$\Phi(\tau) = \lambda^2 \int dk |v(k)|^2 \exp[-i\omega(k)\tau] \qquad (7)$$

is the memory function of the reservoir (continuum). Here, we assume that the solution to the nonlinear Volterra equation [Eq. (6)] with the initial condition $c_a(0)=1$ fully decays toward zero as $t \to \infty$. In the linear Fano-Anderson model, i.e., for $\gamma=0$, the necessary and sufficient condition for the full decay of $c_a(t)$ is the nonexistence of bound states for the full Hamiltonian $H=H_0+\lambda V$ (see, for instance, Refs. 3, 9, 10, 33, and 37). In particular, for a small interaction ($\lambda \to 0$), the full decay of $c_a(t)$ is ensured provided that ω_a is embedded in the continuum (i.e., $\omega_1 < \omega_a < \omega_2$) and that the reservoir spectral function $G(\omega) \equiv \pi |v(\omega)|^2 \rho(\omega)$ [$\rho(\omega) = \partial k / \partial \omega$ is the density of states of the continuum] vanishes at the band edges $\omega = \omega_{1,2}$ (see, for instance, Ref. 37). Unfortunately, in the nonlinear case, it is a challenging task to provide general and rigorous conditions that ensure a full decay of $c_a(t)$; however, this problem goes beyond the purpose of this work.[38] In the next section, it will be shown that, in the $\lambda^2 t$ limit, the dynamics of the survival probability $P(t) = |c_a(t)|^2$ can be derived from a potential and full decay is attained provided that the nonlinear frequency $\omega_a^{NL} = \omega_a - \gamma P$ remains fully inside the band (ω_1, ω_2) of the continuum for $0 \leq P \leq 1$.

B. Nonlinear bound states

Though in the nonlinear regime spectral methods cannot be applied to study the dynamics of Eqs. (4) and (5), it is nevertheless worth to briefly investigate the existence of nonlinear bound states of the nonlinear Fano-Anderson model since they can play an important role in the decay dynamics of $c_a(t)$, as discussed in the next section.

For the nonlinear Fano-Anderson Hamiltonian H, one can introduce nonlinear eigenstates $|\psi_E\rangle$ corresponding to the eigenvalues $E=\hbar\Omega$ as solutions of the nonlinear eigenvalue equation $H|\psi_E\rangle = \hbar\Omega|\psi_E\rangle$. After introduction of the density of states $\rho(\omega) = \partial k / \partial \omega$, from Eqs. (4) and (5), one obtains

$$\Omega c_a = (\omega_a - \gamma |c_a|^2)c_a + \lambda \int_{\omega_1}^{\omega_2} d\omega \sqrt{\rho(\omega)} v(\omega)\tilde{c}(\omega), \quad (8)$$

$$\Omega \tilde{c}(\omega) = \omega \tilde{c}(\omega) + \lambda \sqrt{\rho(\omega)} v^*(\omega) c_a, \qquad (9)$$

where we have set $\tilde{c}(\omega) = \sqrt{\rho(\omega)}c(\omega)$. The nonlinear eigenstate corresponds to a bound state provided that $|\psi_E\rangle$ is square integrable. This implies

$$\|\psi_E\|^2 = |c_a|^2 + \int_{\omega_1}^{\omega_2} d\omega |\tilde{c}(\omega)|^2 < \infty. \qquad (10)$$

Note that, as compared to the linear Fano-Anderson model, the local nonlinearity enters in Eq. (8) to produce a nonlinear shift of the resonance frequency of state $|a\rangle$. As in the linear case (see, for instance, Ref. 39), from Eq. (9), it follows that $\tilde{c}(\omega)$ does not show singularities (i.e., deltalike contributions)—and hence $|\psi_E\rangle$ is square integrable—provided that either Ω falls outside the band (ω_1, ω_2) of the

continuum or Ω falls inside the continuum but $\rho(\omega)|v(\omega)|^2$ vanishes at $\omega = \Omega$ at least as $\sim (\omega - \Omega)^\delta$ for some $\delta > 0$. We therefore have to distinguish two cases.

(*i*) *Bound states outside the continuum.* This is the most common case encountered in a structured continuum with a finite band. A bound state with energy $\hbar\Omega$ outside the continuum exists provided that a root of the equation

$$\Omega - \omega_a + \gamma|c_a|^2 = \lambda^2 \Delta(\Omega) \qquad (11)$$

can be found outside the band (ω_1, ω_2), where we have introduced the energy shift Δ given by

$$\Delta(\Omega) = \int_{\omega_1}^{\omega_2} d\omega \frac{\rho(\omega)|v(\omega)|^2}{\Omega - \omega}. \qquad (12)$$

In the linear case $\gamma=0$, the conditions for the existence of bound states outside the continuum have been widely investigated in the open literature (see, for instance, Refs. 9, 10, and 37). In particular, (i) there can be at most two solutions of Eq. (11) outside the continuum, and a sufficient condition for the existence of two bound states is that $\rho(\omega)|v(\omega)|^2$ does not vanish at the edge of the band, since in this case $\Delta(\Omega)$ diverges to $\mp\infty$ as $\Omega \to \omega_{1,2}^\mp$; (ii) if ω_a falls outside the band (ω_1, ω_2), there is always at least one bound state; and (iii) bound states outside the continuum do not exist provided that $\omega_1 < \omega_a < \omega_2$ and that $\omega_2 - \omega_a > \lambda^2\Delta(\omega_2)$, $\omega_1 - \omega_a < \lambda^2\Delta(\omega_1)$.

In the nonlinear case, note that, if we assume the normalization condition $\|\psi_E\|^2 = 1$, taking into account that $\tilde{c}(\omega) = \lambda \sqrt{\rho(\omega)} v^*(\omega) c_a / (\Omega - \omega)$ [Eq. (9)], from Eqs. (10) and (12), one readily obtains

$$|c_a|^2 = \frac{1}{1 - \lambda^2(d\Delta/d\Omega)}, \qquad (13)$$

and therefore condition (11) for the existence of *nonlinear* bound states outside the continuum is that the equation

$$\Omega - \omega_a = \lambda^2\Delta(\Omega) - \frac{\gamma}{1 - \lambda^2(d\Delta/d\Omega)} \qquad (14)$$

admits solutions outside the band (ω_1, ω_2). Owing to the nonlinear additional term on the right-hand side in Eq. (14), nonlinear bound states may exist in parameter regions where linear bound modes do not exist. For instance, in the $\lambda \to 0$ limit and assuming that $\Delta(\Omega)$ is not singular at the band edges, Eq. (14) yields $\Omega \simeq \omega_a - \gamma$. Therefore, a linear resonance ω_a embedded in the continuum can be shifted outside the band for an enough strong nonlinearity, yielding a bound state outside the continuum. Such a result is well known and has been widely studied, for instance, in tight-binding lattice models with nonlinear impurity modes.[26,34,35] Stability of these nonlinear bound states has also been discussed for some specific models (see, for instance, Ref. 26). Note that, in the $\lambda \to 0$ limit, from Eq. (13), one has $|c_a|^2 \simeq 1$. As the decaying system is initially prepared just in the state $c_a(0) = 1$, the existence of a nonlinear bound state outside the continuum is expected to prevent the decay of $c_a(t)$. As in this work, we are interested to investigate the role of the nonlinearity in the process of the impurity decay dynamics; we will exclude from our analysis the case where the system admits

a bound state outside the continuum. In the $\lambda^2 t$ limit discussed in detail in the next section, it will be shown that the decay of $c_a(t)$ would be prevented owing to the existence of marginally stable bound states outside the continuum when the condition

$$\omega_1 + \gamma < \omega_a < \omega_2 \qquad (15)$$

is not satisfied. Note that the above condition is equivalent to assuming that, during the decay process, the instantaneous nonlinear frequency $\omega_a^{NL} = \omega_a - \gamma P$ of the impurity state always remains embedded in the band (ω_1, ω_2) of the continuum.

(*ii*) *Bound states inside the continuum*. In addition to bound states outside the continuum, in certain special structured reservoirs, there might also exist bound states with energy inside the continuum (see, for instance, Refs. 39 and 40). A nonlinear bound state at frequency Ω embedded in the continuum does exist provided that the following two conditions are simultaneously satisfied:

$$|v(\Omega)|^2 \rho(\Omega) = 0, \quad \Omega - \omega_a + \gamma |c_a|^2 = \lambda^2 \Delta(\Omega). \quad (16)$$

Additionally, $v(\omega)\sqrt{\rho(\omega)}$ should vanish as $\omega \to \Omega$ at least as $\sim(\omega - \Omega)$ in order to ensure a finite norm [Eq. (10)]. The first equation in Eq. (16) can be satisfied for either $\rho(\Omega) = 0$ or $v(\Omega) = 0$. Note that the former case corresponds to the existence of a pointlike gap in the density of states inside the band, whereas the latter case, $v(\Omega) = 0$, implies that the discrete state $|a\rangle$ does not interact with the continuous state of frequency Ω and thus implies a "colored" interaction profile $v(\omega)$ with one zero at $\omega = \Omega$. Though nonlinear bound states embedded in the continuum are expected to be unstable as discussed in the next section, they can nevertheless play a major role in slowing down the decay process of $c_a(t)$. Intuitively, in the regime of a small interaction ($\lambda \to 0$), $|c_a(t)|^2$ varies slowly in time and therefore locally the dynamics of $c_a(t)$ is envisaged to be that of a linear mode with frequency $\omega_a^{NL} = \omega_a - \gamma |c_a(t)|^2$. If in the decay process the amplitude $c_a(t)$ reaches an instantaneous value satisfying Eq. (16), the state of the system is close to the nondecaying nonlinear bound state embedded in the continuum, and therefore the decay is expected to slow down. This dynamical scenario will be described in detail in Sec. IV with reference to a specific lattice model.

III. GRADIENT FLOW DYNAMICS OF THE DECAY IN THE $\lambda^2 t$ LIMIT

A. Multiple-scale asymptotic analysis

In the theory of quantum-mechanical decay of unstable states, a noteworthy limiting case corresponding to an irreversible evolution characterized by a master equation and pure exponential decay is the Van Hove (or $\lambda^2 t$) limit.[2,5,6] The crucial idea is to consider the simultaneous limits $\lambda \to 0$ and $t \to \infty$ with $\lambda^2 t$ finite, i.e., to assume a weak coupling condition ($\lambda \to 0$) and to "observe" the system on the temporal scale $\sim 1/\lambda^2$. It should be noted that, even in the linear case ($\gamma = 0$), an asymptotic analysis of Eqs. (4) and (5) [or of

the eigenvalue equations (8) and (9)] in the $\lambda \to 0$ limit poses severe mathematical difficulties owing to the appearance of resonance singularities (Poincarè resonances) in the series expansion (see, for instance, Refs. 41–43). Though a rigorous approach to overcome the subtle mathematical difficulties arising from resonances would require the introduction of a complex spectral representation for the Hamiltonian, a pure exponential decay (golden-rule result) can be obtained in a simple way in the asymptotic expansion by collecting the most diverging terms in t (the most secular effect) that are precisely characterized by the $\lambda^2 t$ expansion. Following this simpler approach, here we extend the $\lambda^2 t$ limit to investigate the decay dynamics for the nonlinear Fano-Anderson model presented in the previous section. By means of a multiple-scale asymptotic analysis of Eqs. (4) and (5) in the $\lambda \to 0$ limit, a differential equation for $c_a(t)$ is derived as a solvability condition at order $\sim \lambda^2$ in the asymptotic expansion which reproduces the golden-rule result in the linear regime. The problem is to construct an asymptotic approximation for the amplitude $c_a = c_a(t; \lambda)$ as $\lambda \to 0$, with $c_a(0, \lambda) = 1$, which is valid uniformly in time at least up to the Van Hove time scale $\sim 1/\lambda^2$. The choice of the scaling in the asymptotic analysis should be consistent with the Van Hove result that, in the linear $\gamma = 0$ limit, the survival probability $P(t) = |c_a(t)|^2$ must decay exponentially. In order to perform the asymptotic analysis, it is convenient to remove the rapidly varying oscillating term $\sim \exp(-i \int_0^t dt' \omega_a^{NL} dt')$ from the amplitude $c_a(t)$, which survives in the $\lambda = 0$ limit, by the introduction, in place of $c_a(t)$ and $c(k, t)$, of the following amplitudes:

$$C_a(t) = c_a(t) \exp(i\omega_a t) \exp\left[-i\gamma \int_0^t dt' |c_a(t')|^2\right], \quad (17)$$

$$C(k, t) = c(k, t) \exp(i\omega_a t) \exp\left[-i\gamma \int_0^t dt' |c_a(t')|^2\right]. \quad (18)$$

Substitution of Eqs. (17) and (18) into Eqs. (4) and (5) yields the following coupled equations for the amplitudes C_a and C:

$$i\dot{C}_a(t) = \lambda \int dk \, v(k) C(k, t), \qquad (19)$$

$$i\dot{C}(k, t) = [\omega(k) - \omega_a + \gamma |C_a(t)|^2] C(k, t) + \lambda v^*(k) C_a(t). \qquad (20)$$

An inspection of the structure of Eqs. (19) and (20) suggests one to seek for a solution in the form of the following perturbation expansion:

$$C_a = C_a^{(0)} + \lambda^2 C_a^{(2)} + \cdots, \qquad (21)$$

$$C = \lambda C^{(1)} + \lambda^3 C^{(3)} + \cdots. \qquad (22)$$

As we require the asymptotic expansion for C_a to be uniformly valid in time, multiple scales for time are requested to remove secular growing terms that arise in the perturbation expansion as a result of resonance effects. Precisely, we introduce the two times scales

$$T_0 = t, \quad T_2 = \lambda^2 t. \tag{23}$$

As shown below, the evolution of $C_a^{(0)}$ on the time scale T_2 will be derived as a solvability condition in the perturbation analysis at the order $\sim \lambda^2$. To further proceed in the analysis, we must specify the order of magnitude of all the parameters entering in Eqs. (19) and (20) and especially the order of magnitude of the nonlinearity γ. As our aim is to highlight deviations from the exponential decay (golden-rule result) induced by the nonlinearity of the system, we will consider the scaling $(\omega_2 - \omega_1) \sim \gamma \sim 1$ corresponding to a "strong" nonlinear regime. In fact, in this limit, the nonlinearity is strong enough that the deviation of the "nonlinear" resonance frequency ω_a^{NL} from ω_a induced by the nonlinearity is of the same order of magnitude than the bandwidth of the continuum. Introducing *Ansätze* (21) and (22) into Eqs. (19) and (20), using the derivative rule $\partial_t = \partial_{T_0} + \lambda^2 \partial_{T_2}$ and collecting the terms of the same order in the equations so obtained, a hierarchy of equations for successive corrections to C_a and C is obtained. At leading order, $\sim \lambda^0$, from Eq. (19), one simply obtains

$$i \frac{\partial C_a^{(0)}}{\partial T_0} = 0, \tag{24}$$

whose solution is given by

$$C_a^{(0)} = A(T_2), \tag{25}$$

where the amplitude A may vary on the slow time scale T_2 and $A(0) = 1$. At order $\sim \lambda$, from Eq. (20), one has

$$i \frac{\partial C^{(1)}}{\partial T_0} - [\omega(k) - \omega_a + \gamma |A|^2] C^{(1)} = v^*(k) A, \tag{26}$$

whose solution, with the initial condition $C^{(1)}(k,0) = 0$, is given by

$$C^{(1)}(k, T_0) = - i v^*(k) A(T_2) \int_0^{T_0} dt'$$

$$\times \exp[- i \omega(k) t' + i \omega_a t' - i \gamma |A|^2 t']. \tag{27}$$

Finally, at order $\sim \lambda^2$, from Eq. (19), one obtains

$$i \frac{\partial C_a^{(2)}}{\partial T_0} = F(T_0), \tag{28}$$

where the forcing term F is given by

$$F(T_0) = - i \frac{\partial A}{\partial T_2} - i A \int d\omega \rho(\omega) |v(\omega)|^2 \int_0^{T_0} dt'$$

$$\times \exp[- i(\omega - \omega_a + \gamma |A|^2) t']. \tag{29}$$

In order to analyze the occurrence of secular growing terms in the solution $C_a^{(2)}$, which would make the term $\lambda^2 C_a^{(2)}$ in Eq. (21) of the same order as $C_a^{(0)}$ after a time $\sim 1/\lambda^2$, we need to study the behavior for $T_0 \to \infty$ of the forcing term F entering in Eq. (28). Taking into account the well-known relation

$$\lim_{T_0 \to \infty} \int_0^{T_0} dt' \exp[- i(\omega - i0^+) t'] = \pi \delta(\omega) - i \mathcal{P} \left(\frac{1}{\omega} \right), \tag{30}$$

the asymptotic behavior of F at large values of T_0 can be obtained from Eq. (29) and explicitly reads

$$F(T_0) \sim - i \frac{\partial A}{\partial T_2} - i G(\omega_a^{NL}) A + \Delta(\omega_a^{NL}) A, \tag{31}$$

where we have set $\omega_a^{NL} \equiv \omega_a - \gamma |A|^2$ and we introduced the spectral reservoir function G and energy shift Δ according to

$$G(\omega) \equiv \pi \rho(\omega) |v(\omega)|^2, \quad \Delta(\omega) \equiv \mathcal{P} \int d\omega' \frac{\rho(\omega') |v(\omega')|^2}{\omega - \omega'}. \tag{32}$$

In order to avoid the occurrence of a secular growing term on the right-hand side of Eq. (28), we thus require $F(T_0) \sim 0$ as $T_0 \to \infty$, which using Eq. (31) yields

$$\frac{\partial A}{\partial T_2} = - G(\omega_a - \gamma |A|^2) A - i \Delta(\omega_a - \gamma |A|^2) A. \tag{33}$$

Reintroducing the physical time variable t and taking into account that $\partial / \partial t = \partial / \partial T_0 + \lambda^2 \partial / \partial T_2$, one finally obtains $c_a(t) = A(t) \exp[- i \omega_a t + i \int_0^t dt' \gamma |A(t')|^2] + O(\lambda^2)$, where the slow evolution of the amplitude A up to the time scale $\sim 1/\lambda^2$ is ruled by the order parameter equation

$$\frac{dA}{dt} = - \lambda^2 G(\omega_a - \gamma |A|^2) A - i \lambda^2 \Delta(\omega_a - \gamma |A|^2) A. \tag{34}$$

It should be noted that in the linear case ($\gamma = 0$), Eq. (34) leads to an exponential decay for the amplitude $c_a(t)$, with an amplitude decay rate $\lambda^2 G(\omega_a)$ and a frequency shift $\lambda^2 \Delta(\omega_a)$ which are exactly the same as those obtained by the Weisskopf-Wigner approximation. In the nonlinear regime ($\gamma \neq 0$), the extension of the equation has a simple physical explanation: the amplitude A satisfies the same golden-rule equation in which the instantaneous decay rate and frequency shift are calculated at the instantaneous nonlinear frequency $\omega_a^{NL} = \omega_a - \gamma |A(t)|^2$. Note that during the decay, the frequency ω_a^{NL} spans the interval $(\omega_a - \gamma, \omega_a)$ of the continuum, and thus, for a nonflat continuum, the instantaneous decay rate varies during the decay, leading to a nonexponential decay. Since such a nonexponential decay is distinct from the standard corrections occurring in the Zeno or power-law-decay temporal regions, we may refer to it as a nonexponential decay of purely nonlinear nature.

B. Gradient flow dynamics

An important consequence of the $\lambda^2 t$ limit is that the dynamics of the survival probability $P = |A|^2$ can be derived from a potential (or free energy). In fact, from Eq. (34), it can be readily shown that $P(t)$ is governed by the gradient flow

$$\frac{dP}{dt} = -\frac{\partial V}{\partial P}, \qquad (35)$$

where the potential V is given by

$$V(P) = 2\lambda^2 \int_0^P dx\, x G(\omega_a - \gamma x) \qquad (36)$$

and $P(0)=1$. Note that $V(P) \geq 0$ and $V(0)=0$. Since $dV/dt = (\partial V/\partial P)(\partial P/\partial t) = -(\partial V/\partial P)^2 \leq 0$, V is a Lyapunov function and stable fixed points of the dynamics correspond to local minima of V. Note that, since $G \geq 0$ [see Eq. (32)], $V(P)$ is a monotonic increasing function of P. Moreover, since $G(\omega)$ vanishes outside the range (ω_1, ω_2), for P larger than the critical value $P_c = (\omega_a - \omega_1)/\gamma$, the potential $V(P)$ becomes flat.

Owing to the gradient flow dynamics, in the asymptotic $\lambda^2 t$ limit, the necessary and sufficient condition for a full decay of the amplitude c_a is that the potential $V(P)$ shows only one (absolute) minimum at $P=0$ and no plateau regions when P varies in the range $(0,1)$, i.e., that $V(P') > V(P'')$ for any $P', P'' \in (0,1)$ with $P' > P''$. Using Eq. (36), it can be easily shown that such a condition is satisfied provided that $\omega_a < \omega_2$ and $\omega_a > \omega_1 + \gamma$, as anticipated in Sec. II B [see Eq. (15)]. The former condition, $\omega_a < \omega_2$, ensures that $V(P) > V(0)$ for any $P>0$, i.e., the absence of a plateau region around $P=0$. The latter condition, $\omega_a > \omega_1 + \gamma$, ensures that the critical value P_c is larger than 1 so that the plateau region of $V(P)$ for $P > P_c$ is never reached by the dynamics. Note that, as discussed in Sec. II B, breakdown of the condition $\omega_a > \omega_1 + \gamma$ physically corresponds to the appearance of a nonlinear bound state, which would prevent the decay of the impurity state owing to a self-trapping effect as discussed in previous works (see, for instance, Refs. 26, 34, and 35). In our work, we will exclude such a case and will assume a full decay of $c_a(t)$. In order to highlight the role played by the nonlinearity in the decay process, we first recall that in the linear regime ($\gamma=0$), $V(P)$ is parabolic and, provided that $G(\omega_a) \neq 0$, the decay is purely exponential with a decay rate $2\lambda^2 G(\omega_a)$ according to the Fermi golden rule. Conversely, in the nonlinear regime, the decay turns out to deviate from an exponential law provided that $G(\omega)$ is not flat in the spectral range $(\omega_a - \gamma, \omega_a)$, i.e., provided that the reservoir is "structured" in this spectral range. A noteworthy case is that of a structured reservoir showing zeros of the spectral function $G(\omega)$ inside the range $(\omega_a - \gamma, \omega_a)$ (see Fig. 1). If $G(\omega)$ vanishes at the frequencies $\Omega_1, \Omega_2, \ldots, \Omega_N$ inside this range, then the potential V shows horizontal flex points at $P_1 = (\omega_a - \Omega_1)/\gamma$, $P_2 = (\omega_a - \Omega_2)/\gamma, \ldots$, $P_N = (\omega_a - \Omega_N)/\gamma$ which are fixed points of the dynamics. However, they turn out to be unstable. In fact, close to one of such flex points, for example, for $P(t)$ close to P_1, one can approximately set $V(P) \simeq V(P_1) + (\beta/3)(P-P_1)^3$, with $\beta \equiv \lambda^2 \gamma^2 P_1 (\partial^2 G/\partial \omega^2)_{\Omega_1} > 0$, and the dynamics for $\delta P \equiv P(t) - P_1$ is locally described by the equation
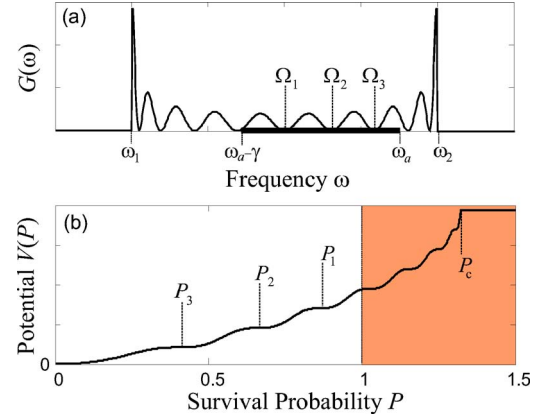

FIG. 1. (Color online) Schematic behavior of a reservoir spectral function $G(\omega)$ for (a) a structured reservoir showing pointlike gaps in the band and (b) corresponding behavior of the potential $V(P)$ governing the gradient flow decay in the $\lambda^2 t$ limit. In (a), the horizontal thick solid line indicates the frequency range $(\omega_a - \gamma, \omega_a)$ spanned by the nonlinear instantaneous frequency $\omega_a^{NL} = \omega_a - \gamma P$ of the impurity mode during the decay process, whereas $\Omega_1, \Omega_2, \ldots$, are the zeros of $G(\omega)$ embedded in this range. In (b), $P_c = (\omega_a - \omega_1)/\gamma$ is the critical value of P above which $V(P)$ = const, $P_1, P_2, \ldots$, are the horizontal flex points of the potential associated with the roots $\Omega_1, \Omega_2, \ldots$, of $G(\omega)$, and the shaded area is a forbidden region of the motion. For $P_c > 1$ as in the figure, starting from the initial condition $P(0)=1$, the globally stable attractor of the flow is $P=0$, whereas the fixed points at the flexes $P_1, P_2, \ldots$, represent unstable trapping states which slow down the decay of the survival probability $P(t)$.

$$\frac{d\delta P}{dt} = -\beta(\delta P)^2, \qquad (37)$$

whose solution explicitly reads

$$\delta P(t) = \frac{\delta P(0)}{\beta \delta P(0)t + 1}. \qquad (38)$$

Therefore, for $\delta P(0) > 0$, i.e., if $P(t)$ approaches the fixed point P_1 from above, one has $\delta P(t) \to 0$ and $P(t)$ is attracted toward P_1, leading to a freezing of the decay. Conversely, for $\delta P(0) < 0$, i.e., if $P(t)$ is close to the fixed point P_1 from below, $P(t)$ goes away from P_1 due to the divergence at $t = -1/[\beta \delta P(0)]$ in Eq. (38). The fixed point $P = P_1$ is therefore one-sided unstable. Note that in the decay dynamics of the survival probability $P(t)$, the fixed point P_1 is always approached from above, so that the decay is strongly slowed down in the vicinity of P_1. A small perturbation in the system, such as noise, may trigger $P(t)$ below P_1 for an infinitesimal quantity, and hence may push $P(t)$ away from P_1 and restart the decay until the next one-sided unstable fixed point P_2 is reached, and so on. Therefore, for a structured reservoir showing zeros of the spectral function $G(\omega)$, the decay of the survival probability $P(t)$ is expected to show a characteristic staircase shape, with decay slowing down and transient trapping in proximity of the flex points of the potential $V(P)$. This dynamical behavior will be confirmed by direct numerical simulations in case of a tight-binding lattice model,
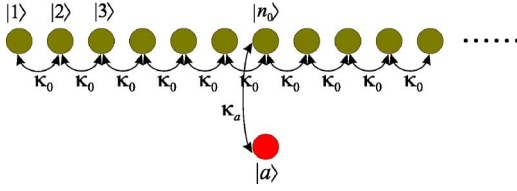
FIG. 2. (Color online) Schematic of a nonlinear site $|a\rangle$ side coupled to a semi-infinite tight-binding lattice. κ_0 is the hopping amplitude between adjacent sites in the lattice, whereas κ_a is the hopping amplitude between the localized state $|a\rangle$ and the site $|n_0\rangle$ of the lattice.

which is described in the next section. It is finally worth pointing out that the slowing down of the decay at points $P_1, P_2, \ldots, P_N$ corresponds to the state of the system approaching a nonlinear bound state embedded in the continuum, which therefore acts as an unstable attractor of the dynamics. In fact, in the $\lambda \to 0$ limit, we can neglect in the second equation of Eq. (16) the $\lambda^2 \Delta(\Omega)$ term, which is of order $\sim \lambda^2$. A nonlinear bound state embedded in the continuum thus corresponds to a frequency Ω_l, which is a root of the reservoir spectral function $G(\omega)$ [first equation in Eq. (16)], and, in addition, requires an occupation probability $P_l = |c_a|^2$ at the impurity satisfying the condition $\Omega_l - \omega_a + \gamma P_l \simeq 0$ [second equation in Eq. (16)], that is, $P_l = (\omega_a - \Omega_l)/\gamma$.

IV. DECAY OF A NONLINEAR IMPURITY SITE IN A SEMI-INFINITE TIGHT-BINDING LATTICE

In this section, we apply the general results derived in the previous section to a one-dimensional tight-binding lattice with a nonlinear impurity site, which provides a rather simple realization of the Fano-Anderson model[33] with a local nonlinear state and that may describe electron- or photon-transport phenomena in condensed-matter or photonic tight-binding lattices. Our model is a variant of similar lattice models considered in recent works (see, for instance, Refs. 18, 19, 25, 26, 29, 30, 35, and 36) and has been introduced in Ref. 44 as an example of colored Fano-Anderson model supporting bound states embedded in the continuum. The system consists of a single nonlinear state $|a\rangle$ side coupled to a semi-infinite linear tight-binding lattice in the geometry depicted in Fig. 2. The nonlinear state $|a\rangle$ is tunneling coupled to the site $|n_0\rangle$ of the chain ($n_0 \geq 1$) with an hopping amplitude κ_a, whereas the hopping amplitude of adjacent sites $|n\rangle$ and $|n \pm 1\rangle$ in the lattice is denoted by κ_0. The tight-binding lattice provides the continuum of width $4\kappa_0$ in which the state $|a\rangle$ may decay. Indicating by c_n ($n \geq 1$) the occupation amplitude of site $|n\rangle$ in the semi-infinite lattice and by c_a the occupation amplitude of the impurity site $|a\rangle$, in the nearest-neighbor tight-binding approximation, the equations of motion for c_n and c_a read

$$i\dot{c}_n = -\kappa_0(c_{n+1} + c_{n-1}) - \kappa_a c_a \delta_{n,n_0} \quad (n \geq 2), \qquad (39)$$

$$i\dot{c}_1 = -\kappa_0 c_2 - \kappa_a c_a \delta_{n_0,1}, \qquad (40)$$

$$i\dot{c}_a = \omega_a c_a - \kappa_a c_{n_0} - \gamma|c_a|^2 c_a, \qquad (41)$$

where ω_a is the offset of the (linear) resonance frequency of the impurity site $|a\rangle$ from the center of the tight-binding lattice band, and γ is the nonlinear parameter. Note that in the Wannier basis $|n\rangle$, Eqs. (39)–(41) can be derived from the tight-binding Hamiltonian

$$H_{TB} = -\hbar \sum_{n=1}^{\infty} \kappa_0(|n\rangle\langle n+1| + |n+1\rangle\langle n|)$$
$$+ \hbar(\omega_a - \gamma|c_a|^2)|a\rangle\langle a| - \hbar\kappa_a(|a\rangle\langle n_0| + |n_0\rangle\langle a|). \qquad (42)$$

Introducing the continuous Bloch states $|k\rangle$ of the semi-infinite lattice by the relation

$$|k\rangle = \sum_{n=1}^{\infty} \sqrt{\frac{2}{\pi}} \sin(nk)|n\rangle, \qquad (43)$$

with $0 < k < \pi$, it can be readily shown that in the basis $\{|k\rangle, |a\rangle\}$ the tight-binding Hamiltonian [Eq. (42)] assumes the nonlinear Fano-Anderson form of Sec. II [see Eqs. (1)–(3)], with

$$\omega(k) = -2\kappa_0 \cos k, \qquad (44)$$

$$\lambda v(k) = -\sqrt{\frac{2}{\pi}} \kappa_a \sin(n_0 k). \qquad (45)$$

Note that, if time is normalized to $1/\kappa_0$, the coupling of site $|a\rangle$ with the continuum scales as $\sim (\kappa_a/\kappa_0)$, and therefore one can assume $\lambda \equiv (\kappa_a/\kappa_0)$ as the measure of the interaction strength. Note also that the density of states $\rho(\omega) = \partial k/\partial \omega$ and the reservoir spectral function $G(\omega) = \pi\rho(\omega)|v(\omega)|^2$ for this model explicitly read

$$\rho(\omega) = \frac{1}{\sqrt{4\kappa_0^2 - \omega^2}}, \qquad (46)$$

$$G(\omega) = \frac{2\kappa_0^2}{\sqrt{4\kappa_0^2 - \omega^2}} \sin^2\left[n_0 \arccos\left(\frac{\omega}{2\kappa_0}\right)\right]. \qquad (47)$$

Before proceeding into the study of the decay dynamics of the impurity site in the nonlinear regime, it is worth discussing the decay process in the linear regime, which is attained by setting $\gamma = 0$ in the Hamiltonian [Eq. (42)].

A. Decay dynamics in the linear regime

In the linear regime, model (42) is a generalization of the well-known tight-binding Fano-Anderson model with a constant interaction coupling $v(k) = \text{const}$,[33] and basically reduces to it in the limit $n_0 \to \infty$ (see Ref. 44). Lattice truncation introduces a colored interaction between the impurity site and the semi-infinite tight-binding lattice which is responsible for novel features in the decay dynamics as compared to the uncolored case of Ref. 33 even in the linear regime. Here, we present the main results concerning the

linear decay dynamics of the impurity site in presence of such a colored interaction.[44]

(*i*) *Basic equations.* In the linear regime, the decay law for the amplitude $c_a(t)$ can be derived in an analytical form using standard spectral methods (see, for instance, Refs. [2], [3], and [33]). If we denote by $\hat{c}_a(s) = \int_0^\infty dt c_a(t)\exp(-st)$ [$\mathrm{Re}(s) > 0$] the Laplace transform of $c_a(t)$, one has $\hat{c}_a(s) = i/[is - \omega_a - \lambda^2 \Sigma(s)]$ and hence, after inversion,

$$c_a(t) = \frac{1}{2\pi} \int_{0^+ - i\infty}^{0^+ + i\infty} ds \frac{\exp(st)}{is - \omega_a - \lambda^2 \Sigma(s)}, \quad (48)$$

where $\Sigma(s)$ is the self-energy given by

$$\Sigma(s) = \int dk \frac{|v(k)|^2}{is - \omega(k)} = \frac{1}{\pi} \int_{\omega_1}^{\omega_2} d\omega \frac{G(\omega)}{is - \omega}. \quad (49)$$

Possible poles on the imaginary axis of $\hat{c}_a(s)$ correspond to bound states of H and are responsible for fractional decay of the amplitude $c_a(t)$. In fact, using the property

$$\Sigma(s = -i\omega \pm 0^+) = \Delta(\omega) \mp iG(\omega), \quad (50)$$

the poles $s_p = -i\Omega$ of $\hat{c}_a(s)$ satisfy the conditions $\Omega - \omega_a = \lambda^2 \Delta(\Omega)$ and $G(\Omega) = 0$, i.e., they correspond to bound states (either outside or inside the continuum) of H. In absence of poles (i.e., of bound states of H), $c_a(t)$ decays to zero, whereas in presence of poles, Eq. (48) can be written as the sum of a contour (decaying) integral plus the (nondecaying) pole contributions. Using Eqs. (44), (45), and (49), the self-energy $\Sigma(s)$ can be calculated in an exact form and reads

$$\Sigma(s) = \frac{2\kappa_0^2}{\pi} \int_0^\pi dk \frac{\sin^2(n_0 k)}{is + 2\kappa_0 \cos k}$$

$$= -\frac{i\kappa_0^2}{\sqrt{s^2 + 4\kappa_0^2}} \left[1 - \left(\frac{i\sqrt{s^2 + 4\kappa_0^2} - is}{2\kappa_0} \right)^{2n_0} \right]. \quad (51)$$

Using Eq. (50), the following expression for $\Delta(\omega) = \mathrm{Re}[\Sigma(s = -i\omega \pm 0^+)]$ can then be derived:

$$\Delta(\omega) = \begin{cases} -\dfrac{\kappa_0^2}{\sqrt{\omega^2 - 4\kappa_0^2}} \left[1 - \left(\dfrac{\sqrt{\omega^2 - 4\kappa_0^2} + \omega}{2\kappa_0} \right)^{2n_0} \right], & \omega < -2\kappa_0 \\[4mm] \dfrac{\kappa_0^2}{\sqrt{4\kappa_0^2 - \omega^2}} \sin\left[2n_0 \cos^{-1}\left(\dfrac{\omega}{2\kappa_0} \right) \right], & -2\kappa_0 < \omega < 2\kappa_0 \\[4mm] \dfrac{\kappa_0^2}{\sqrt{\omega^2 - 4\kappa_0^2}} \left[1 - \left(\dfrac{\sqrt{\omega^2 - 4\kappa_0^2} - \omega}{2\kappa_0} \right)^{2n_0} \right], & \omega > 2\kappa_0. \end{cases} \quad (52)$$

Note the oscillatory behavior of both $G(\omega)$ and $\Delta(\omega)$, with the existence of $(2n_0 - 1)$ zeros of $\Delta(\omega)$ at $\omega_l = -2\kappa_0 \cos[l\pi/(2n_0)]$ ($l = 1, 2, \ldots, 2n_0 - 1$) and of $(n_0 + 1)$ zeros of $G(\omega)$ at $\omega_m = -2\kappa_0 \cos(m\pi/n_0)$ ($m = 0, 1, 2, \ldots, n_0$). Note, in particular, that, for $n_0 \geq 2$, there are $(n_0 - 1)$ frequencies Ω_l ($l = 1, 2, \ldots, n_0 - 1$), embedded in the continuum and given by

$$\Omega_l = -2\kappa_0 \cos(l\pi/n_0) \quad (l = 1, 2, \ldots, n_0 - 1), \quad (53)$$

in correspondence of which the reservoir spectral function G vanishes.

(*ii*) *Bound states outside the continuum.* At most, two bound states at frequency Ω outside the band $(-2\kappa_0, 2\kappa_0)$ from either sides may exist. Precisely, a bound state at frequency $\Omega > 2\kappa_0$ exists provided that $2\kappa_0 - \omega_a < \lambda^2 \Delta(2\kappa_0)$, i.e., $\omega_a > 2\kappa_0 - \kappa_a^2 n_0/\kappa_0$, whereas a bound state at frequency $\Omega < -2\kappa_0$ does exist for $-2\kappa_0 - \omega_a > \lambda^2 \Delta(-2\kappa_0)$, i.e., for $\omega_a < -2\kappa_0 + \kappa_a^2 n_0/\kappa_0$. Therefore, if the frequency ω_a of the discrete level lies inside the interval

$$-1 + \frac{\kappa_a^2 n_0}{2\kappa_0^2} < \frac{\omega_a}{2\kappa_0} < 1 - \frac{\kappa_a^2 n_0}{2\kappa_0^2}, \quad (54)$$

bound states outside the continuum do not exist. For a given value of n_0, Eq. (54) is satisfied for a sufficiently small value of the coupling $\lambda = \kappa_a/\kappa_0$ and provided that the frequency ω_a is not too close to the band edges. In the following, it will be assumed that no bound states exist outside the continuum.

(*iii*) *Bound states inside the continuum.* According to Eq. (16) with $\gamma = 0$, one linear bound state embedded in the continuum for the model expressed by Eqs. (44) and (45) exists at $\Omega = \Omega_l$ for any $n_0 \geq 2$, provided that the frequency ω_a of the impurity site assumes one of the following $(n_0 - 1)$ allowed values:

$$\omega_a = \Omega_l - \lambda^2 \Delta(\Omega_l) = -2\kappa_0 \cos(l\pi/n_0) \quad (l = 1, 2, \ldots, n_0 - 1). \quad (55)$$

From a physical viewpoint, the bound state embedded in the continuum corresponds, in the Wannier state representation [Eq. (42)], to localization at sites $|1\rangle, |2\rangle, \ldots, |n_0 - 1\rangle$, and $|a\rangle$,

i.e., to $c_n=0$ for $n \geq n_0$ (see Ref. 44 for more details).

(iv) *Decay dynamics and fractional decay due to bound states embedded in the continuum.* Suppose that H_{TB} does not admit bound states. The amplitude $c_a(t)$ given by Eq. (48) then decays toward zero as $t \to \infty$. After a suitable deformation in the complex plane of the contour for the integral on the right-hand side of Eq. (48), the amplitude $c_a(t)$ can be written in the form (see Ref. 44)

$$c_a(t) = \frac{1}{2\pi}\left(\frac{\kappa_a}{\kappa_0}\right)^2 \int_0^\pi dk \frac{\sin^2(n_0 k)\exp(2i\kappa_0 t \cos k)}{[\omega_a/(2\kappa_0) + \cos k - (\kappa_a/2\kappa_0)^2 \sin(2n_0 k)/\sin k]^2 + [\kappa_a^2/(2\kappa_0^2)]^2 \sin^4(n_0 k)/\sin^2 k}. \tag{56}$$

On the time scale corresponding to the Van Hove $\lambda^2 t$ limit, $c_a(t)$ decays exponentially with a decay rate $2\lambda^2 G(\omega_a)$. Nonexponential features in the decay are visible, as usual, on the short and long time scales solely (see, for instance, Fig. 4 to be discussed later). Conversely, if H_{TB} admits of one bound state embedded in the continuum, $\hat{c}_a(s)$ has one pole on the imaginary axis at $s_p = -i\omega_a$, and the integral in Eq. (48) comprises, in addition to a decaying term, an oscillatory (nondecaying) term arising from the pole contribution to the integral, namely, one has

$$c_a(t) = c_{pole}(t) + c_{decay}(t), \tag{57}$$

where the pole contribution is given by

$$c_{pole}(t) = \frac{\exp(-i\omega_a t)}{1 + \dfrac{n_0}{2}\left(\dfrac{\kappa_a}{\kappa_0}\right)^2\left[1 - \left(\dfrac{\omega_a}{2\kappa_0}\right)^2\right]^{-1/2}}, \tag{58}$$

whereas the decay contribution $c_{decay}(t)$ is given by the same expression appearing on the right-hand side of Eq. (56) (the integral should now be taken as a principal value). The existence of a bound state embedded in the continuum is thus responsible for a fractional decay of the amplitude $c_a(t)$.

B. Nonlinear decay dynamics

Let us consider now the role of the nonlinearity on the decay dynamics of the impurity site. The main features of the nonlinear decay dynamics in the Van Hove limit, predicted in Sec. III, are (i) the appearance of nonexponential deviations of the decay law of purely nonlinear nature related to a colored spectral reservoir function and (ii) the slowing down of the decay due to an unstable self-trapping mechanism when the system gets close to a nonlinear bound state embedded in the continuum.

To check these predictions, we numerically integrated Eqs. (39)–(41) by an accurate fourth-order Runge-Kutta method with variable step. In the numerical analysis, the semi-infinite lattice has been truncated at some finite integer n (typically $n=100$), and a smooth absorbing boundary condition at the boundary has been assumed to avoid spurious reflections due to lattice truncation. This was simply achieved by the introduction of smoothly increasing fictitious loss terms in Eq. (39) close to the truncation site number. We first considered the decay dynamics in the $n_0=1$ case, i.e., for a structured continuum which does not support bound states inside the continuum. A detailed analysis of the decay law P for this case has been recently given in Refs. 17 and 18 in the linear regime ($\gamma=0$). Figure 3 shows a typical example of the decay dynamics as obtained in the nonlinear regime. Figures 3(a) and 3(b) show the behavior of the reservoir spectral function $G(\omega) = \pi\rho(\omega)|v(\omega)|^2$ and corresponding potential $V(P)$ governing the relaxational dynamics. The solid curve in Fig. 3(c) shows the behavior of the survival probability $P(t) = |c_a(t)|^2$ versus time as obtained by the numerical simulations of Eqs. (39)–(41) with initial conditions $c_a(0)=1$ and $c_n(0)=0$. The dotted line in the figure, almost overlapped with the solid one, shows the corresponding behavior of $P(t)$ as predicted by the gradient flow [Eq. (35)], i.e., in the $\lambda^2 t$ limit. In order to highlight the deviations of $P(t)$ from a pure exponential decay law, we calculated the behavior of the instantaneous decay rate $\alpha(t) = -(\ln P)/t$ versus time, which is shown in the inset of Fig. 3(c). Note that $\alpha(t) \to 0$ as $t \to 0$, which is related to the parabolic behavior of $P(t)$ close to $t=0$ (Zeno region). Such a behavior is obviously not predicted within the $\lambda^2 t$ limit, and, in fact, the solid and dotted curves in the inset of Fig. 3(c) deviate for times shorter than ~ 20. After this Zeno region, the behavior of $\alpha(t)$ is well reproduced by the gradient flow dynamics, at least up to $t \sim 200$.[45] Note that, in this intermediate temporal region, $\alpha(t)$ is not constant, as one would expect for a linear system; therefore, in this temporal region, there is a clear signature of deviations from an exponential decay of *purely nonlinear nature*. We checked this point by direct numerical simulations of Eqs. (39)–(41) for the same parameter values as in Fig. 3, but assuming a linear impurity mode ($\gamma=0$). The behaviors of the survival probability $P(t)$ and corresponding instantaneous decay rate $\alpha(t) = -(\ln P)/t$ in this case are shown in Fig. 4. Note that, in the intermediate temporal region separating the Zeno region ($t \sim 20$) and the oscillatory power-law-decay region ($t \sim 200$, see note 45, $\alpha(t)$ turns out to be almost flat and equal to the golden-rule decay rate represented by the dotted horizontal curve.

For $n_0 \geq 2$, the reservoir spectral function $G(\omega)$ shows pointlike gaps in the lattice transmission band, so that the decay of the impurity mode $|a\rangle$ may be slowed down via the trapping mechanism discussed in Sec. III B. Figure 5 shows a typical example of the decay dynamics corresponding to $n_0=8$. For parameter values used in the simulations, there are three roots of the reservoir spectral function inside the range
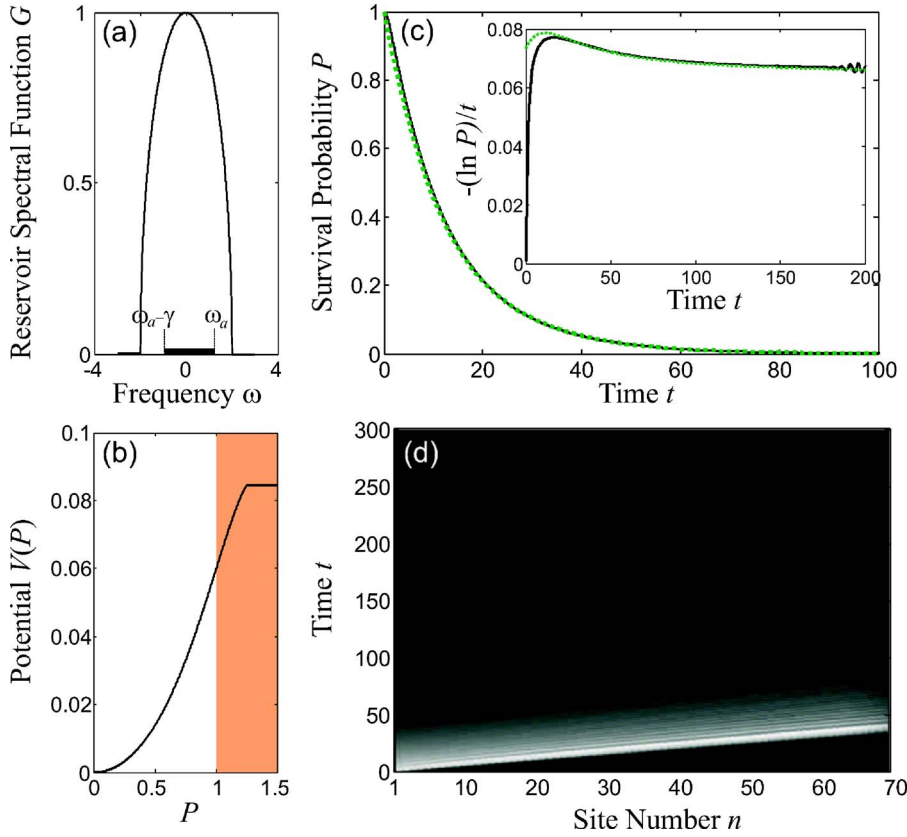
FIG. 3. (Color online) Decay dynamics of the nonlinear site $|a\rangle$ in the lattice model of Fig. 2 for $n_0=1$ and for $\omega_a=1.2$, $\kappa_0=1$, $\kappa_a=0.2$, and $\gamma=2$. (a) Behavior of the reservoir spectral function G, as given by Eq. (47). (b) Behavior of the potential $V(P)$ [Eq. (36)]. (c) Behavior of the survival probability $P(t)=|c_a(t)|^2$ versus time as computed by numerical simulations of Eqs. (39)–(41) (solid curve), and corresponding behavior as predicted by the gradient flow [Eq. (35)] (dotted line, almost overlapped with the solid curve). The inset shows the behavior of the instantaneous decay rate $\alpha(t)=-[\ln P(t)]/t$ versus time. (d) Grayscale image showing the temporal evolution of the occupation probabilities $|c_n(t)|^2$ at the lattice sites.

$(\omega_a-\gamma,\omega_a)$, which correspond to three unstable trapping states for the potential $V(P)$ [see Figs. 5(a) and 5(b)]. The behavior of the survival probability $P(t)$ as obtained by numerical simulations of Eqs. (39)–(41), together with the behavior of the instantaneous decay rate $\alpha(t)=-(\ln P)/t$, is shown in Fig. 5(c). Note that the decay shows a characteristic staircase profile, with slowing down of the decay in correspondence of the three trapping states as indicated by the arrows in the figure. The trapping time at each flex point of the potential $V(P)$ turns out to be sensitive to the noise in the

system, especially for the trapping states closer to $P=0$; in the simulations shown in Figs. 5(c) and 5(d), it is just the "numerical noise" introduced by the discretization procedure to trigger the instability from one unstable trapping state to the next one.[46] Note that the trapping time increases at successive steps [i.e., from (1) to (3) in Fig. 5(c)] because the successive horizontal flex points of the potential $V(P)$ encountered during the decay get flatter [see Fig. 5(b)]. The staircase shape of the decay law is clearly evidenced in Fig. 5(d) by the appearance of successive radiation bursts which propagate away from the site $|n_0\rangle$ of the lattice toward the sites $n>n_0$. Note that the transient localization at sites $1\leq n\leq n_0-1$ between successive radiation bursts is the clear signature that the system is close to an unstable bound state embedded in the continuum.

V. CONCLUSIONS

In this work, the decay dynamics of a nonlinear impurity mode embedded in a linear structured continuum has been theoretically investigated in the framework of a nonlinear generalization of the Fano-Anderson model. In the Van Hove $(\lambda^2 t)$ limit, it has been shown by means of a multiple-scale asymptotic analysis that the decay dynamics for the survival probability can be derived from a potential V (gradient flow) and that full decay is attained provided that the nonlinear resonance frequency of the impurity mode remains within the continuum during the decay. Deviations of the potential V from a parabola, which generally occur for a structured
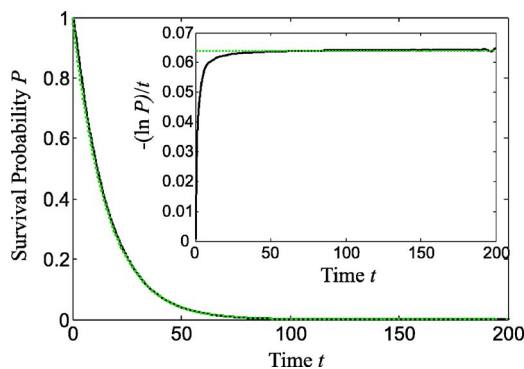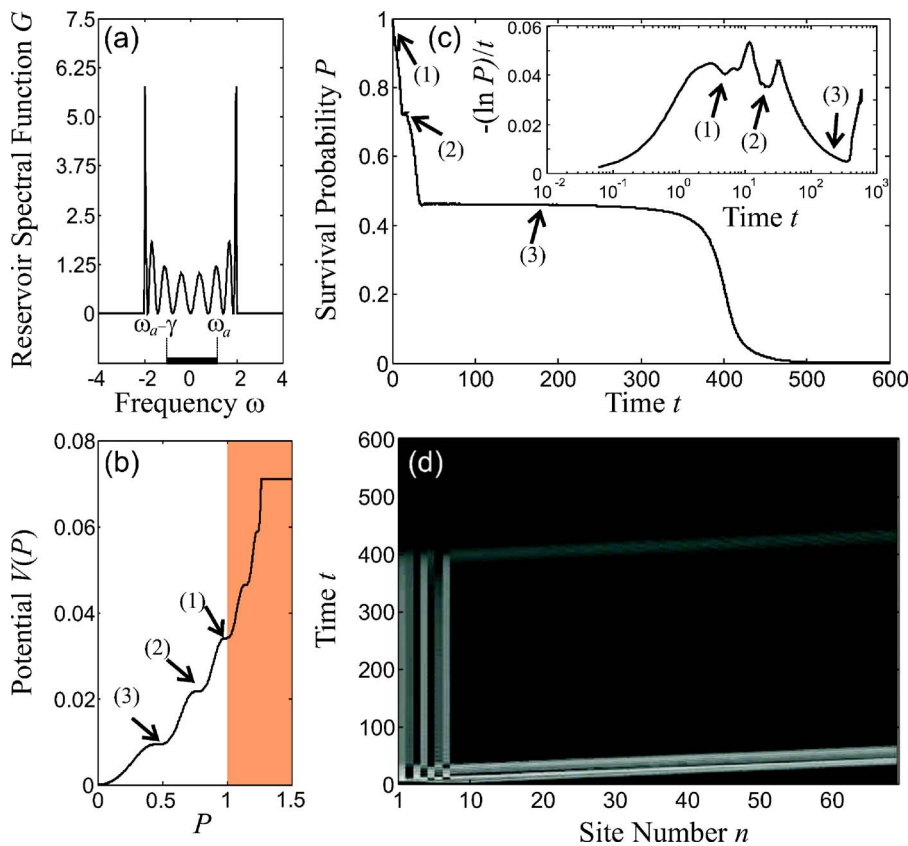

FIG. 4. (Color online) Decay dynamics of the survival probability $P(t)=|c_a(t)|^2$ of state $|a\rangle$ in the linear regime. Parameter values are the same as in Fig. 3 except for $\gamma=0$. The inset shows the behavior of the instantaneous decay rate $\alpha(t)=-[\ln P(t)]/t$ versus time. Solid and dotted curves refer to the results as obtained by numerical simulations of Eqs. (39)–(41) and by the gradient flow [Eq. (35)], respectively.

FIG. 5. (Color online) Same as Fig. 3 but for $n_0=8$. For the sake of clearness, in the inset in (c), the horizontal time scale is logarithmic. The arrows in the figures correspond to slowing down of the decay associated with the three flex points (1), (2), and (3) of the potential V.

reservoir, are responsible for the appearance of nonexponential features in the decay law of purely nonlinear nature. In particular, for structured reservoirs showing pointlike gaps in the band, a trapping mechanism which slows down the decay has been predicted and related to the existence of bound states embedded in the continuum. Such a dynamical behavior has been specifically studied for a simple tight-binding one-dimensional lattice model with a nonlinear impurity site, which may describe electron or photon transport in condensed matter or photonic systems. Numerical simulations of the underlying equations confirm, in particular, the appearance of nonexponential features of purely nonlinear nature and the slowing down of the decay via unstable trapping states.

[1] L. Fonda, G. C. Ghirardi, and A. Rimini, Rep. Prog. Phys. **41**, 587 (1978).

[2] H. Nakazato, M. Namiki, and S. Pascazio, Int. J. Mod. Phys. B **10**, 247 (1996).

[3] C. Cohen-Tannoudji, J. Dupont-Roc, and G. Grynberg, *Atom-Photon Interactions* (Wiley, New York, 1992).

[4] P. Facchi and S. Pascazio, in *Quaderni di Fisica Teorica*, edited by S. Boffi (Bibliopolis, Napoli, 1999).

[5] L. Van Hove, Physica (Amsterdam) **21**, 517 (1955).

[6] P. Facchi and S. Pascazio, Physica A **271**, 133 (1999).

[7] A. G. Kofman and G. Kurizki, Nature (London) **405**, 546 (2000).

[8] S. John and J. Wang, Phys. Rev. Lett. **64**, 2418 (1990).

[9] A. G. Kofman, G. Kurizki, and B. Sherman, J. Mod. Opt. **41**, 353 (1994).

[10] P. Lambropoulos, G. M. Nikolopoulos, T. R. Nielsen, and S. Bay, Rep. Prog. Phys. **63**, 455 (2000).

[11] P. Lodahl, A. F. van Driel, I. S. Nikolaev, A. Irman, K. Overgaag, D. Vanmaekelbergh, and W. L. Vos, Nature (London) **430**, 654 (2004).

[12] M. Razavy, *Quantum Theory of Tunneling* (World Scientific, River Edge, NJ, 2003).

[13] S. R. Willkinson, C. F. Bharucha, M. C. Fischer, K. W. Madison, P. R. Morrow, Q. Niu, B. Sundaram, and M. G. Raizen, Nature (London) **387**, 575 (1997).

[14] M. C. Fischer, B. Gutierrez-Medina, and M. G. Raizen, Phys. Rev. Lett. **87**, 040402 (2001).

[15] A. Barone, G. Kurizki, and A. G. Kofman, Phys. Rev. Lett. **92**, 200403 (2004).

[16] G. Hackenbroich, B. Rosenow, and H. A. Weidenmuller, Phys. Rev. Lett. **81**, 5896 (1998).

[17] E. Rufeil Fiori and H. M. Pastawski, Chem. Phys. Lett. **420**, 35 (2006).

[18] S. Longhi, Phys. Rev. Lett. **97**, 110402 (2006); Phys. Rev. E **74**, 026602 (2006).

[19] S. Longhi, Phys. Rev. A **74**, 063826 (2006).

[20] F. S. Cataliotti, S. Burger, C. Fort, P. Maddaloni, F. Minardi, A. Trombettoni, A. Smerzi, and M. Inguscio, Science **293**, 843 (2001).

[21] C. Bruder, R. Fazio, and G. Schön, Ann. Phys. **14**, 566 (2005).

[22] O. Morsch and M. Oberthaler, Rev. Mod. Phys. **78**, 179 (2006).

[23] V. M. Kenkre and D. K. Campbell, Phys. Rev. B **34**, 4959 (1986).

[24] D. Chen, M. I. Molina, and G. P. Tsironis, J. Phys.: Condens. Matter **5**, 8689 (1993).

[25] M. I. Molina and G. P. Tsironis, Phys. Rev. B **47**, 15330 (1993).

[26] M. I. Molina, Phys. Rev. B **71**, 035404 (2005).

[27] D. N. Christodoulides, F. Lederer, and Y. Silberberg, Nature (London) **424**, 817 (2003).

[28] L. Hadzievski, A. Maluckov, M. Stepic, and D. Kip, Phys. Rev. Lett. **93**, 033901 (2004).

[29] A. E. Miroshnichenko, S. F. Mingaleev, S. Flach, and Yu. S. Kivshar, Phys. Rev. E **71**, 036626 (2005).

[30] A. E. Miroshnichenko and Y. S. Kivshar, Phys. Rev. E **72**, 056611 (2005).

[31] C. R. Rosberg, D. N. Neshev, W. Krolikowski, A. Mitchell, R. A. Vicencio, M. I. Molina, and Yu. S. Kivshar, Phys. Rev. Lett. **97**, 083901 (2006).

[32] U. Fano, Phys. Rev. **124**, 1866 (1961).

[33] G. D. Mahan, *Many-Particle Physics* (Plenum, New York, 1990), pp. 272–285.

[34] M. I. Molina, Phys. Rev. B **67**, 054202 (2003).

[35] M. I. Molina, R. A. Vicencio, and Y. S. Kivshar, Phys. Lett. A **350**, 134 (2006).

[36] A. E. Miroshnichenko, M. I. Molina, and Y. S. Kivshar, Phys. Rev. E **75**, 046602 (2007).

[37] B. Gaveau and L. S. Schulman, J. Phys. A **28**, 7359 (1995).

[38] Sufficient conditions for the stability of the zero solution of nonlinear integrodifferential Volterra equations based on a Lyapunov functional analysis have been given by Burton [see T. A. Burton, *Volterra Integral and Differential Equations* (Academic, New York, 1983); J. Math. Anal. Appl. **85**, 90 (1982)]; however, these conditions seem either too cumbersome or too restrictive to be applied to our physical model.

[39] M. Miyamoto, Phys. Rev. A **72**, 063405 (2005).

[40] G. Sudarshan, in *Field Theory, Quantization and Statistical Physics*, edited by E. Tirapegui (Reidel, Dordrecht, 1981), pp. 237–245.

[41] T. Petrosky, I. Prigogine, and S. Tasaki, Physica A **173**, 175 (1991).

[42] I. Prigogine, Phys. Rep. **219**, 93 (1992).

[43] E. C. G. Sudarshan, C. B. Chiu, and G. Bhamathi, Physica A **202**, 540 (1994).

[44] S. Longhi, arXiv:quant-ph/0612152 (unpublished).

[45] At longer times, $P(t) \ll 1$ and the nonlinearity of the impurity state can be neglected; therefore, the long-time asymptotic decay law for $P(t)$ is of oscillatory power-law type (see, for instance, Ref. 18), a feature which is not accounted for in the $\lambda^2 t$ limit. A signature of the long-time power-law decay is the appearance of oscillations in the behavior of $\alpha(t)$ at times t larger than ~ 200 in the insets of Figs. 3(c) and 4.

[46] For this reason, a quantitative comparison of the decay law as predicted by Eqs. (39)–(41) and by the gradient flow [Eq. (35)] is in this case not reliable.